Misbinding of color and motion in human early visual cortex: Evidence from event-related potentials

Yanyu Zhang [a,b,c,d], Xilin Zhang [a,b,c,d], Yizhou Wang [e], Fang Fang [a,b,c,d,*]

[a] D   d   (d   ),   ,   1006s71,
[b]   d   ,   ,   1006s71,   ,   1006s71,
[c]   -   ,   ,   1006s71,   ,
[d]   - D /   ,   ,   ,   1006s71,
[e]   d   ,   ,   d   ,   ,   ,   1006s71,

ABSTRACT

One of the central tasks for the visual system is to integrate visual features into objects, which is referred to as the binding problem. To study the binding mechanisms, it has been suggested to use phenomena of feature misbinding to separate active feature binding from feature co-occurence. Taking advantage of a steady-state misbinding of color and motion, we performed psychophysical and event-related potential (ERP) adaptation experiments to investigate the neural mechanisms of the misbinding (i.e., the active color-motion binding). Human subjects adapted to the misbinding of color and motion, as well as their correct binding that was used for identifying neural processes associated with the co-occurrence of color and motion. We found that adaptation to the misbinding and the correct binding could generate color-contingent motion aftereffects (CCMAEs), but in opposite directions. ERP adaptation effects manifested in the earliest ERP component C1. The C1 latency in the misbinding condition was 11 ms longer than that in the correct binding condition. In the correct binding condition, the C1 adaptation effect (i.e., the C1 amplitude reduction after adaptation) took place in the peak phase of the C1. The dipole source of the adaptation effect was located in V1. In the misbinding condition, the C1 adaptation effect occurred in the descending phase of the C1 and its dipole source was in V2. In both conditions, the C1 adaptation effects correlated with the CCMAEs across individual subjects. These findings provide human electro-physiological evidence that active feature binding takes place in early visual cortex, but at later processing stages than feature co-occurrence.

© 2016 Elsevier Ltd. All rights reserved.

1. Introduction

Different visual features (e.g., color, motion, and orientation) of an object are processed to a certain degree by different functional specialized modules of cerebral cortex. For example, some V4 neurons respond selectively to color, and V5 neurons encode various aspects of motion information (Fellaman & Van Essen, 1991; Livingstone & Hubel, 1988). However, we perceive coherent objects, rather than their isolated components, such as colors, orientations, and shapes. To achieve a unitary percept, the visual system must integrate the activity of these functional modules and link visual features belonging to the same object, which is known as the binding problem. This becomes very difficult when multiple objects appear simultaneously in the visual field because the visual system needs to assign the correct color, motion, and orientation to each object.

The binding problem is one of the most puzzling and interesting issues that cognitive neuroscience has ever faced. Numerous theo-

cortex has been suggested to be involved in the reentrant processes, as evidenced by functional magnetic resonance imaging (fMRI), transcranial magnetic stimulation (TMS), and neuropsychological studies (Colby & Goldberg, 1999; Esterman, Verstynen, & Robertson, 2007; Friedman-Hill, Robertson, & Treisman, 1995; Koivisto & Silvanto, 2012; Robertson, 2003; Shafritz, Gore, & Marois, 2002) showing that this area could modulate feature binding but had little influence on feature detection. Besides the binding mechanism at a relatively late stage of visual information processing, some researchers proposed that binding could also take place at an early stage of visual processing, even in the absence of attention. Their conjecture is mainly based on psychophysical findings on rapid feature integration (Bodelón, Fallah, & Reynolds, 2007; Holcombe & Cavanagh, 2001) and visual contingent aftereffects (Humphrey & Goodale, 1998; Wolfe & Cave, 1999). It is known that visual contingent aftereffects are confined to the position of adaptation (Gibson & Radner, 1937; Stromeyer, 1972), that there is a lack of interocular transfer (Mayhew & Anstis, 1972), and that they could be induced by adaptation to locally paired dots that moved in opposite directions (Blaser, Papathomas, & Vidnyánszky, 2005). These findings are taken as evidence for early binding mechanisms that are dependent on spatial and/or temporal proximity of visual features.

Although significant progress has been made in understanding the binding mechanism, we still know little about its neural implementation. Furthermore, there is a notable shortcoming of most previous studies for addressing the binding problem. In these studies, visual features were presented simultaneously and superimposed. Many neurons in almost all visual cortical areas are now known to code features in multiple dimensions. For example, many color sensitive neurons in V2 are jointly selective for other features, such as motion direction and size (Gegenfurtner, Kiper, & Fenstemaker, 1996). Therefore, the reported binding effects could be ascribed to the physical co-occurrence of features and the sensory representation of feature pairing. It is difficult to know whether the mechanism normally responsible for active feature binding (i.e., perceptual binding) is actually recruited (Di Lollo, 2012; Whitney, 2009).

To address the issues raised above, it is necessary to test conditions in which features are perceptually misbound and investigate how misbinding is realized in the brain, because it is likely that feature misbinding provides the strongest evidence for the existence of the active binding mechanism (Treisman & Schmidt, 1982). Wu, Kanai, and Shimojo (2004) described a vivid and compelling illusion demonstrating a steady-state misbinding of color and motion, which provided a powerful tool to investigate the neural mechanisms of feature misbinding. In a recent study (Zhang, Qiu, Zhang, Han, & Fang, 2014), we used a slightly modified version of their illusion. Our stimulus (Fig. 1A, the left panel) consisted of two sheets of isoluminant dots. One sheet moved up and the other one moved down. On both sheets, dots in the right end (right of the white dashed line, the effect part) and those in the rest area (the induction part) were rendered in different colors (red or green). Oppositely moving dots always had different colors. Thus, the induction and effect parts of the stimuli combined color and motion in opposite fashions. Interestingly, when fixating at the center of the stimuli, during most of the viewing time, observers
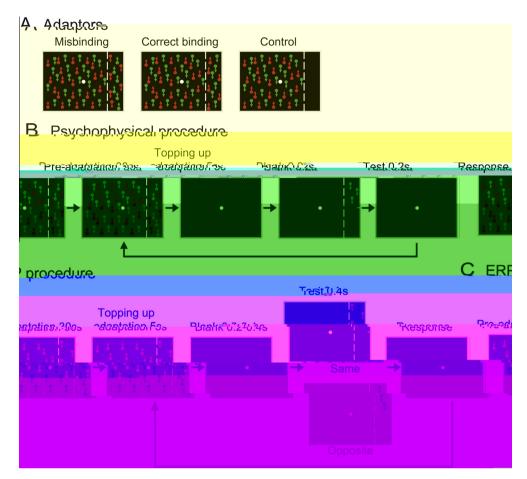
Fig. 1. Visual stimuli and experimental procedures. (A) Adaptors in the misbinding, correct binding, and control conditions. In the misbinding and correct binding conditions, adaptors contain both the induction part and the effect part, which are on the left and the right of the white dashed line, respectively. The dashed line is for illustration purposes only, which was not shown in the experiments. Adaptors in the control condition contain the induction part only. (B) Procedure of the psychophysical experiment. (C) Procedure of the ERP experiment. The same and opposite trials are illustrated here.

two adaptors, dots in the right end area (5.9° × 26.8°, effect part) and those in the rest area (23.6° × 26.8°, induction part) were rendered with different colors, either red (CIE (1931): x = 0.614, y = 0.344) or green (CIE (1931): x = 0.289, y = 0.593). For one adaptor, dots in the effect and induction parts of the upward-moving sheet were red and green, respectively. Dots in the corresponding parts of the downward-moving sheet were green and red, respectively. For the other adaptor, dots in the effect and induction parts of the upward-moving sheet were green and red, respectively. Dots in the corresponding parts of the downward-moving sheet were red and green, respectively. These two adaptors could induce the color-motion misbinding in the effect part. In the correct binding condition (Fig. 1A, the middle panel), the adaptors were identical to those in the misbinding condition except that, on both sheets of the adaptors, dots in the effect part and those in the induction part had the same color. The correct binding condition was included here for identifying neural processes associated with co-occurrence of color and motion. In the control condition (Fig. 1A, the right panel), the two adaptors contained the induction part only. The adaptors were counterbalanced in terms of color-motion pairing. The control condition was used as a baseline for measuring the CCMAEs in the misbinding and the correct binding conditions.

In the psychophysical experiment, there were 10 test stimuli. They were red or green dots presented in the upper half of the effect part area, with one of five different speeds (0.6°/s upward, 0.3°/s upward, 0°/s, 0.3°/s downward, 0.6°/s downward). In the

ERP experiment, for each adaptor, there were two test stimuli, each of which contained both red and green dots moving in opposite directions. The dots in a test stimulus moved in the same or opposite direction to those in the effect part of the adaptor. Throughout the experiments, a white dot was presented at the display center and subjects needed to fixate on it.

2.4.

Using a method of constant stimuli, the psychophysical experiment was designed to measure the CCMAE in the three adaptation conditions. The experiment consisted of 60 blocks of 40 trials, 10 blocks for each adaptor. Each block started with a 30-sec pre-adaptation (Fig. 1B). On a trial, a test stimulus was presented for 0.2 s after a 5 s topping-up adaptation and a 0.2 s blank interval, and subjects made a 2-AFC judgment on the motion direction of the test stimulus (upward or downward). For each adaptor, each of the ten test stimuli was presented on 40 trials. The order of the three adaptation conditions/blocks was randomized across subjects.

2.5. d

We first constructed a psychometric function for each adaptation condition shown in Fig. 2A. We plotted the percentage of trials on which the test stimulus direction was perceived to be opposite to the physical direction of adapting dots (with the same color as
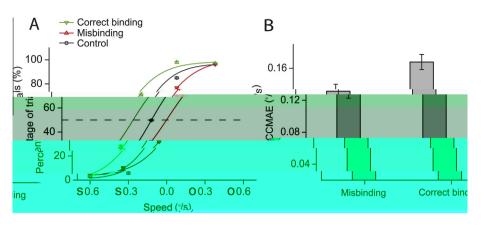
Fig. 2. Psychophysical results. (A) Psychometric functions showing motion direction judgments in the correct binding, misbinding, and control conditions. The abscissa refers to the speed (0, 0.3, or 0.6°/s) and motion direction (S, same; O, opposite) of test stimuli. S and O indicate that the moving direction of a test stimulus was the same as or opposite to that of the adapting dots in the effect part (with the same color as the dots in the test stimulus). The ordinate refers to the percentage of trials in which subjects indicated that the moving direction of a test stimulus was opposite to the physical direction of the adapting dots. (B) The CCMAE magnitudes in the correct binding and misbinding conditions. Error bars denote 1 SEM calculated across subjects.

the test) as a function of the test speed. For each condition, the psychometric values at the five test speeds were fit with a cumulative normal function. We interpolated the data to find the speed expected to be perceived as stationary. The speed difference between the misbinding condition and the control condition was the CCMAE from adaptation to the color-motion misbinding in the effect part, and the speed difference between the correct binding condition and the control condition was the CCMAE from adaptation to the correct color-motion binding.

2.6.

The ERP experiment aimed to measure the color-contingent motion adaptation effect in the brain. It consisted of 36 blocks of 36 trials, 6 blocks for each adaptor. Similar to the psychophysical experiment, each block started with a 30 s pre-adaptation (Fig. 1C). On a trial, after a 5-sec topping-up adaptation and a 0.2–0.4 s blank interval, a test stimulus was presented for 0.4 s. Subjects needed to make a 2-AFC judgment on a near-threshold luminance change (increment or decrement) of the test stimulus for attentional control. The luminance change occurred between 0.2 and 0.4 s after the onset of the test stimulus. It was determined by QUEST staircases (Watson & Pelli, 1983) before the experiment to ensure that subjects performed equally well for all the adapting and test stimuli (75% correct). For each adaptor, each of the two test stimuli was presented on 108 trials. The order of the three adaptation conditions/blocks was randomized across subjects.

2.7. d

EEG was recorded from 64 scalp sites using Ag/AgCl electrodes mounted in an elastic cap (Brain Products, Munich, Germany) according to the extended international 10–20 EEG system. We recorded VEOG (vertical electro-oculogram) from an electrode positioned above the right eye and HEOG (horizontal electro-oculogram) from an electrode at the outer canthus of the left eye. The signals from the 64 scalp electrodes were referenced online to an electrode on the tip of the nose and were re-referenced offline to the mean signal from the left and right mastoids. Impedance for all the electrodes was kept below 5 kΩ. EEG was amplified with a gain of 500 K, band-pass filtered from 0.05 to 100 Hz, and digitized at a sampling rate of 1000 Hz.

2. d

We used Brain Vision Analyzer (Brain Products, Munich, Germany) to analyze EEG signals induced by the test stimuli. EEG data were first low-pass filtered at 30 Hz and then epoched from 100 ms before stimulus onset to 250 ms after stimulus onset. EEG epochs were corrected for baseline over the 100 ms interval immediately before stimulus onset. Eye-blink artifacts were semi-automatically corrected using the method proposed by Gratton, Coles, and Donchin (1983). Any epoch exceeding ±50 μV at any electrode was excluded from analysis. Remaining epochs were selectively averaged according to the types of the test stimuli in which the red and green dots moved in the same (i.e., the same trial) or opposite (i.e., the opposite trial) direction to those in the effect part of the adaptor.

The C1 response was apparent between 60 and 100 ms after stimulus onset. To select electrodes for C1 amplitude and latency analysis, for each adaptation condition, grand averaged ERPs were made by averaging across subjects and test stimuli. Left posterior electrodes, including P1, P3, P5, PO3, PO7, POZ, O1, and Oz, had the largest C1 amplitudes, in all the three adaptation conditions. To calculate the C1 amplitude for each subject, the mean amplitude of the seven sampling points around the C1 peak was first calculated for each of these eight electrodes, and this mean was then averaged across the eight electrodes. The C1 latency was the mean of the C1 peak latencies across these eight electrodes.

To assess differences between the ERP waveforms for the same and opposite trials, we used a criterion of at least 22 consecutive data points (i.e., 22 ms) that are different at a $p < 0.01$ level (paired t-test for difference of means). A similar criterion was used by Murray et al. (2002). They used 11 consecutive data points at a 500 Hz digitization rate. Here, we used 22 consecutive data points at a 1000 Hz digitization rate, which means the same length of data points as that in Murray et al.'s study. Using the method proposed by Guthrie and Buchwald (1991), we calculated the corrected p-value of <0.018.

To measure the C1 adaptation effect in each adaptation condition, we computed an adaptation index I_A to quantify how much the C1 response changed after adaptation relative to the overall response to the stimuli. In the misbinding and correct binding conditions, the index was defined as $(A_{same} - A_{opposite})/(A_{same} + A_{opposite})$, where A_{same} and $A_{opposite}$ are the mean C1 amplitudes on the same and opposite trials, respectively. Generally, the larger the absolute value of the index, the greater the C1 adaptation effect.

2. .

Estimation of dipole sources was performed using the Brain Electrical Source Analysis (BESA) algorithm (BESA version 5.3). For the misbinding and correct binding conditions, dipole modeling was carried out based on the difference waveforms between the same and opposite trials. We first used one dipole with free location and orientation to fit the distribution of the difference waveform in the 68–110 ms interval for the misbinding condition and in the 57–79 ms interval for the correct binding condition, respectively. The four-shell ellipsoidal head model was used. The initial starting position of the dipole was randomly chosen and using different starting locations yielded a highly similar dipole configuration. Then, we localized a dipole within area V1 to best account for the distribution of the difference waveform in the 68–110 ms interval for the misbinding condition and a dipole within area V2 to best account for the distribution of the difference waveform in the 57–79 ms interval for the correct binding condition, respectively.

3. Results

3.1.

In the psychophysical experiment, we measured the CCMAE from adapting to the correct binding or the misbinding of color and motion in the effect part. After pre-adaptation and topping-up adaptation, a test stimulus (i.e., red or green moving dots) was presented briefly, and subjects made a 2-AFC judgment on the motion direction of the test stimulus (upward or downward) (Fig. 1B).

Because data from the red and green test stimuli showed a similar pattern, they were pooled together for analysis. Fig. 2A shows the psychometric functions in the three adaptation conditions. In the control condition, subjects adapted to the induction part only. Their performance was almost perfect for all the test stimuli (about 50% level for the $0°/s$ stimulus, good judgment for the $0.3°/s$ and $0.6°/s$ stimuli), demonstrating that adaptation to the induction part only generated little CCMAE in the effect part area. However, after adapting to the correct binding of color and motion, the psychometric function showed a leftward shift. This result demonstrated that subjects' perception of the moving direction of the tests was biased opposite to the physical direction of the adapting dots (with the same color as the test). Strikingly, after adapting to the misbinding of color and motion, the psychometric function exhibited a rightward shift, showing that subjects' perception of the direction of the tests was biased opposite to the perceived (rather than the physical) direction of the adapting dots. These results demonstrated that adaptation to the color-motion misbinding could generate the CCMAE and the CCMAEs in the misbinding and the correct binding conditions had opposite directions, suggesting that neurons in visual cortex might represent the color-motion misbinding for the dots in the effect part.

To quantitatively measure the CCMAE magnitude in each adaptation condition, psychometric values at the five test speeds were fit with a cumulative gaussian function. We interpolated the data to find the speed expected to be perceived stationary. We used the speed in the control condition as a baseline. The speed differences between the control condition and the correct binding condition (mean ± SEM: $0.17 ± 0.01°/s$) and between the control condition and the misbinding condition (mean ± SEM: $0.13 ± 0.01°/s$) were defined as the CCMAE magnitudes in the correct binding condition and the misbinding condition, respectively (Fig. 2B). Both the CCMAE magnitudes were significantly above zero (both $t(23) > 14.94$, $p < 0.001$). The CCMAE magnitude

in the correct binding condition was significantly greater than that in the misbinding condition ($t(23) = 8.11$, $p < 0.001$).

3.2.

The ERP experiment aimed to measure the color-contingent motion adaptation effect in the brain. The experimental protocol (Fig. 1C) in the ERP experiment was similar to that of the psychophysical experiment except that subjects were asked to make a 2-AFC judgment on a near-threshold luminance change of the test stimulus (200–400 ms after stimulus onset). The test stimuli were different from those in the psychophysical experiment. There were two test stimuli for each adaptor. Each test contained both red and green dots. In one test, the dots were identical to those in the effect part of the adaptor, whereas the dots in the other test moved in opposite directions to those in the effect part of the adaptor. They performed equally well (about 75% correct) across the three adaptation conditions and the two types of trials. ERPs evoked by the test stimuli on the same and opposite trials were analyzed. The C1 was visible between 50 and 110 ms after stimulus onset (Fig. 3A). Left posterior electrodes, including P1, P3, P5, PO3, PO7, POZ, O1, and Oz, had the largest C1 amplitudes in the three adaptation conditions (Fig. 3B and C). Statistical analyses were based on the averages of the C1 amplitudes and latencies across these eight electrodes. We hypothesize that, if the C1 component is associated with the misbinding of color and motion, according to the ERP adaptation logic (Hoffmann, Unsöld, & Bach, 2001), the C1 component on the same trials should be larger than that on the opposite trials. On the other hand, if the C1 component is also associated with the correct binding of color and motion, the C1 component should show an opposite pattern. Based on previous neurophysiological and fMRI findings (Gegenfurtner et al., 1996; Zhang et al., 2014), we further hypothesize that the adaptation effects on the C1 component in the misbinding and correct binding conditions might take place in different phases of this component.

Fig. 3A shows the averaged waveforms across the eight electrodes and all subjects in the three adaptation conditions. In the misbinding condition, the peak amplitude of the C1 component was larger on the same trials than that on the opposite trials ($t(21) = 2.68$, $p < 0.05$). In contrast, in the correct binding condition, the peak amplitude of the C1 component was smaller on the same trials than that on the opposite trials ($t(21) = 2.70$, $p < 0.05$). In the control condition, there was no significant amplitude difference between the two types of trials ($t(21) = 0.27$, $p > 0.79$). For the peak latency of the C1 component, there was no significant difference between the same and opposite trials in all the three conditions (all $t(21) < 1.94$, $p > 0.07$). The peak latencies of the C1 components (averaged across the same and opposite trials) in the misbinding, correct binding, and control conditions were 79, 68, and 69 ms, respectively. A one-way repeated-measures ANOVA of C1 peak latency revealed a significant main effect of adaptation condition ($F(2,42) = 17.14$, $p < 0.001$). Post hoc paired t-tests showed that the C1 peak latency in the misbinding condition was significantly longer than those in the correct binding and the control conditions (misbinding vs. correct binding: $t(21) = 5.29$, $p < 0.001$; misbinding vs. control: $t(21) = 5.88$, $p < 0.001$). But there was no significant difference between the correct binding and control conditions.

A closer look at the ERP waveforms in Fig. 3A revealed that the differences between the same and opposite trials were not limited to the C1 peak amplitudes and latencies. We further assessed the ERP waveform differences between the same and opposite trials. The gray shaded areas in Fig. 3A show the intervals (i.e., time points) with significant amplitude difference between the same and opposite trials ($p < 0.01$, paired t-test at 22 consecutive time points). For the misbinding condition, significant difference was found in the descending phase of the C1 component

(68–110 ms after stimulus onset). However, for the correct binding condition, the C1 peak phase (57–79 ms after stimulus onset) exhibited significant difference. No significant difference was found in the control condition.
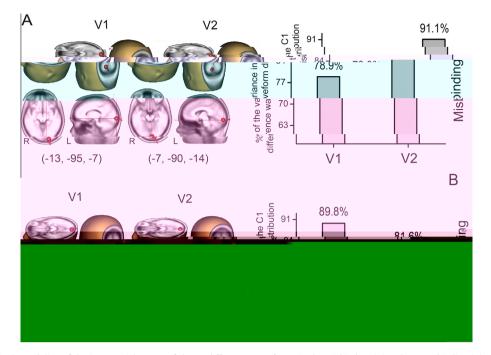
3.3. D   d

Fig. 4. Dipole modeling of the intracranial source of the C1 difference waveforms in the misbinding (A) and correct binding (B) conditions.

psychophysical and ERP experiments. The CCMAE was significantly correlated with the C1 adaptation index in both the misbinding ($r = 0.451$, $p = 0.035$) and correct binding ($r = -0.478$, $p = 0.024$) conditions (Fig. 5). Note that, according to the definition of the C1 adaptation index (see the method part), in the misbinding condition, the stronger the adaptation effect, the most positive the index, resulting a positive correlation coefficient. However, in the correct binding condition, the stronger the adaptation effect, the more negative the index, resulting a negative correlation coefficient.

4. Discussion

Using psychophysical and ERP adaptation techniques, our study provides the following findings on the mechanisms of the color-motion misbinding. (1) Adaptation to the color-motion misbinding could generate a CCMAE. The direction of the CCMAE followed the prediction by the misbinding, opposite to the CCMAE direction from adaptation to the correct binding. This finding replicated our previous work (Zhang et al., 2014). (2) The peak latency of the C1 components induced by the test stimuli after adapting to the misbinding was about 11 ms later than that after adapting to the correct binding. (3) The reduced C1 amplitude (i.e., the C1 adaptation effect) after adapting to the correct binding manifested in the peak phase of the C1 component, whereas the reduction after adapting to the misbinding manifested in the descending phase of the C1 component. (4) The C1 adaptation effects were closely associated with the CCMAEs in both the correct binding and the misbinding conditions. (5) The dipole source analysis showed that the C1 adaptation effects in the correct binding and the misbinding conditions reflected neural adaptation in V1 and V2, respectively. These results suggest that both the correct binding and the misbinding take place in early visual cortex, but at different levels of the visual processing hierarchy.

It should be noted that the C1 adaptation effects cannot be explained by attention. Subjects were asked to perform a near-threshold luminance change task with the test stimuli for attentional control. They performed equally well for all the adaptors and test stimuli, presumably holding effort and attention constant across all the conditions. Moreover, luminance changes occured between 200 and 400 ms after the onset of the test stimuli. EEG signals in this interval were notintemluded for analysis.

Fig. 5. Correlations between the CCMAE magnitude and the C1 adaptation effect across individual subjects in the misbinding (A) and correct binding (B) conditions.

Electrophysiological studies in monkey subjects have found that color and motion are processed in different, yet mutually connected cortical pathways (Fellaman & Van Essen, 1991). It is widely accepted that the color processing pathway consists of the blobs of V1, the thin stripes of V2, and V4, and the motion processing pathway includes the layer 4B of V1, the thick stripes of V2, and V5/MT+ (Bartels & Zeki, 2000; Sincich & Horton, 2005). Meanwhile, neurons selective for both color and motion direction were found in V1 (Gegenfurtner et al., 1996). Recently, using fMRI, Seymour, Clifford, Logothetis, and Bartels (2009) applied multivariate pattern analysis (MVPA) to decode subjects' perception when they viewed color-motion conjunctions. It was shown that the physical feature conjunctions could be decoded from fMRI spatial activation patterns in early visual cortical areas, as early as in V1. This finding demonstrated an explicit representation of feature conjunctions at early visual processing stages, consistent with our finding in the correct binding condition. It is very likely that prolonged viewing of the correct binding of color and motion had adapted the dually selective neurons for color and motion direction in V1. This is why we found the C1 adaptation effect in the peak phase of the C1 component. Our finding here and Seymour et al.'s finding might imply an early mechanism of visual feature conjunction. However, these findings cannot inform us whether the conjunction representation in early visual areas is the sensory coding of a feature pairing or the perceptual readout of a binding operation. We still do not know whether an active feature binding mechanism is indeed recruited for these unambiguous visual stimuli in these studies. Thus, to reveal the binding mechanisms, it is necessary to use visual stimuli that can induce feature misbinding.

Dually selective neurons for color and motion direction were much more common in V2 than V1 (Tamura, Sato, Katsuyama, Hata, & Tsumoto, 1996). Furthermore, Shipp, Adams, Moutoussis, and Zeki (2009) reported that such neurons are found more frequently in the superficial and deep layers (1, 2, 5, and 6) that receive feedback modulations from V4 and V5, relative to the intermediate layers (3 and 4) that relay ascending feedforward signals. We recently found that, after viewing the color-motion misbinding, the fMRI adaptation effect in V2 was closely associated with the CCMAE (Zhang et al., 2014). Furthermore, effective connectivity analyses showed that enhanced cortical feedback from V4 to V2 and from V5 to V2 might contribute to the misbinding. Our results in the misbinding condition are in line with these neurophysiological, anatomical, and fMRI findings. First, the peak latency of the C1 components in the misbinding condition was about 11 ms later than that in the correct binding condition. Second, the C1 adaptation effect in the misbinding condition was found in the descending phase of the C1 component, and the cortical source of the adaptation effect was identified in V2. These two findings may reflect the later activation of neurons in the feedback layers of V2 by the test stimuli in the misbinding condition, relative to the neuronal activation in V1 by the test stimuli in the correct binding condition (Girard, Hupe, & Bullier, 2001).

In sum, the current study provides human electrophysiological evidence that active feature binding takes place in early visual cortex, but at later processing stages than feature co-occurrence. It complements and corroborates our previous fMRI findings. In the future, other misbinding and active binding phenomena can be probed to fully understand how the binding problem is solved, which is a key component of visual information processing.

Acknowledgments

References

Ales, J. M., Yates, J. L., & Norcia, A. M. (2010). V1 is not uniquely identified by polarity reversals of responses to upper and lower visual field stimuli. , 52 (4), 1401–1409.

Bartels, A., & Zeki, S. (2000). The architecture of the colour centre in the human visual brain: New results and a review. , 12, 172–193.

Blaser, T., Papathomas, Z., & Vidnyánszky, Z. (2005). Binding of motion and colour is early and automatic. , 21, 2040–2044.

Bodelón, C., Fallah, M., & Reynolds, J. H. (2007). Temporal resolution for the perception of features and conjunctions. , 27(4), 725–730.

Bouvier, S., & Treisman, A. (2010). Visual feature binding requires reentry. , 21, 200–204.

Chen, J., He, Y., Zhu, Z., Zhou, T., Peng, Y., Zhang, X., et al. (2014). Attention-dependent early cortical suppression contributes to crowding. , 34(32), 10465–10474.

Clark, V. P., & Hillyard, S. A. (1996). Spatial selective attention affects early extrastriate but not striate components of the visual evoked potential. , 387–402.

Colby, C. L., & Goldberg, M. E. (1999). Space and attention in parietal cortex. w , 22(1), 319–349.

Di Lollo, V. (2012). The feature-binding problem is an ill-posed problem. d , 16, 317–321.

Esterman, M., Verstynen, T., & Robertson, L. C. (2007). Attenuating illusory binding with TMS of the right parietal cortex. , 35(3), 1247–1255.

Fellaman, D. J., & Van Essen, D. C. (1991). Distributed hierarchical processing in the primate visual cortex. , 1, 1–47.

Foxe, J. J., & Simpson, G. V. (2002). Flow of activation from V1 to frontal cortex in humans: A framework for defining "early" visual processing. , 142, 39–150.

Friedman-Hill, S. R., Robertson, L. C., & Treisman, A. (1995). Parietal contributions to visual feature binding: Evidence from a patient with bilateral lesions. , 26 (5225), 853–855.

Gegenfurtner, K. R., Kiper, D. C., & Fenstemaker, S. B. (1996). Processing of color, form, and motion in macaque are V2. , 13, 161–172.

Gibson, J. J., & Radner, M. (1937). Adaptation, after-effect and contrast in the perception of tilted lines. , 20, 453–467.

Girard, P., Hupe, J. M., & Bullier, J. (2001). Feedforward and feedback connections between areas V1 and V2 of the monkey have similar rapid conduction velocities. 5(3), 1328–1331.

Gratton, G., Coles, M. G., & Donchin, E. (1983). A new method for off-line removal of ocular artifact. d , 55(4), 468–484.

Guthrie, D., & Buchwald, J. S. (1991). Significance testing of difference potentials. , 240–244.

Hoffmann, M. B., Unsöld, A. S., & Bach, M. D. (2001). Directional tuning of human motion adaptation as reflected by the motion VEP. , 41(17), 2187–2194.

Holcombe, A. O., & Cavanagh, P. (2001). Early binding of feature pairs for visual perception. , 4, 127–128.

Humphrey, G. K., & Goodale, M. A. (1998). Probing unconscious visual processing with the McCollough effect. d , 7, 494–519.

Jeffreys, D. A., & Axford, J. G. (1972). Source locations of pattern-specific components of human visual evoked potentials. I. Component of striate cortical origin. , 16, 1–21.

Koivisto, M., & Silvanto, J. (2011). Relationship between visual binding, reentry and awareness. d , 20(4), 1293–1303.

Koivisto, M., & Silvanto, J. (2012). Visual feature binding: The critical time windows of V1/V2 and parietal activity. , 5 , 1608–1614.

Livingstone, M., & Hubel, D. (1988). Segregation of form, color, movement & depth: Anatomy, physiology and perception. , 240, 740–749.

Mayhew, J. W., & Anstis, S. M. (1972). Movement aftereffects contingent on color, intensity, and pattern. & , 12(1), 77–85.

Murray, M. M., Wylie, G. R., Higgins, B. A., Javitt, D. C., Schroeder, C. E., & Foxe, J. J. (2002). The spatiotemporal dynamics of illusory contour processing: Combined high-density electrical mapping, source analysis, and functional magnetic resonance imaging. , 22(12), 5055–5073.

Robertson, L. C. (2003). Binding, spatial attention and perceptual awareness. w , 4(2), 93–102.

Seymour, K., Clifford, C. W., Logothetis, N. K., & Bartels, A. (2009). The coding of color, motion, and their conjunction in the human visual cortex. , 1 (3), 177–183.

Shafritz, K. M., Gore, J. C., & Marois, R. (2002). The role of the parietal cortex in visual feature binding. d d , (16), 10917–10922.

Shipp, S., Adams, D. L., Moutoussis, K., & Zeki, S. (2009). Feature binding in the feedback layers of area V2. , 1 , 2230–2239.

Sincich, L. C., & Horton, J. C. (2005). Input to V2 thin stripes arises from V1 cytochrome oxidase patches. , 25, 10087–10093.

Stromeyer, C. F. (1972). Contour-contingent color aftereffects: Retinal area specificity. , 227–235.

Tamura, H., Sato, H., Katsuyama, N., Hata, Y., & Tsumoto, T. (1996). Less segregated processing of visual information in V2 than V1 of the monkey visual cortex. , 300–309.

Treisman, A. (1996). The binding problem. , *6*(2), 171–178.

Treisman, A., & Schmidt, H. (1982). Illusory conjunctions in the perception of objects. , *14*(1), 107–141.

Watson, A. B., & Pelli, D. G. (1983). QUEST: A Bayesian adaptive psychometric method. *&* , *33*(2), 113–120.

Whitney, D. (2009). Neuroscience: Toward unbinding the binding problem. , *1* , 251–253.

Wolfe, J. M., & Cave, K. R. (1999). The psychophysical evidence for a binding problem in human vision. , *24*(11–17), 111–125.

Wu, D. A., Kanai, R., & Shimojo, S. (2004). Vision: Steady-state misbinding of colour and motion. , *42* , 262.

Zhang, X., Qiu, J., Zhang, Y., Han, S., & Fang, F. (2014). Misbinding of color and motion in human visual cortex. , *24*(12), 1354–1360.

Zhang, X., Zhaoping, L., Zhou, T., & Fang, F. (2012). Neural activities in V1 create a bottom-up saliency map. , *73*(1), 183–192.